

THE DEVELOPMENT OF A FLEXIBLE ROTOR ACTIVE MAGNETIC BEARING SYSTEM

E.O. Ranft*, G. van Schoor* and J.G. Roberts**

* School of Electrical, Electronic and Computer Engineering, North-West University, Potchefstroom Campus, Private Bag X6001, Potchefstroom, 2520, South Africa

**School of Mechanical Engineering, North-West University, Potchefstroom Campus, Private Bag X6001, Potchefstroom, 2520, South Africa

Abstract: A design process comprising aspects of modelling and analysis is developed, implemented and verified for a flexible rotor active magnetic bearing system. The system is specified to experience the first three critical frequencies up to an operating speed of 10,000 rpm. Rotor stability at critical frequencies places specific constraints on the equivalent stiffness and damping parameters of the active magnetic bearing. An iterative design process is then initiated by an electromagnetic design of the radial active magnetic bearings resulting in parameters used in the detailed modelling of the system. Stiffness and damping parameters as well as system dynamic response are verified and used to design a flexible rotor. The magnetic bearing locations, displacement sensor locations and rotordynamic response are verified using finite element analysis. The design of the rotor stands central to the iterative design process since it impacts on the forces experienced by the active magnetic bearings as well as the critical frequencies of the active magnetic bearing system. Once constructed the actual active magnetic bearing system stiffness and damping parameters as well as dynamic response are compared to modelled results. The rotordynamic response is characterised by measuring the rotor displacement at pre-defined locations as the rotor traverses the critical frequencies. These results are compared with the predicted rotordynamic response.

Key words: Active magnetic bearing, design process, flexible rotor, rotordynamic analysis.

1. INTRODUCTION

Active magnetic bearings (AMBs) have a number of novel qualities rendering them invaluable machine components in the modern day industry. Their ability to suspend a rotor without mechanical contact results in a no wear and no lubrication configuration. This renders the AMB an environmentally friendly technology [1].

One application that stands to benefit from AMB technology is the Pebble Bed Modular Reactor (PBMR) currently in development in South Africa. According to Shi et al. [2] AMBs will become largely conventional in this application. Shi et al. [2] and Takizuka et al. [3] both conducted various studies on AMBs with the aim of applying them in high temperature reactor (HTR) facilities.

The need exists to establish a knowledge base on AMBs for the industry from which AMBs can be specified, implemented and maintained. Discussions with industry highlighted rotordynamic performance of an AMB suspended rotor as one of the key areas of research. An AMB suspended flexible rotor design process must be developed, implemented and verified.

2. DESIGN PROCESS

The iterative design process outlined in Figure 1 shows

the first step as a complete system specification. From the system specification a maximum bearing load capacity along with a force slew rate are estimated and used to conduct a preliminary analytical electromagnetic (EM) design. Parameters obtained from the EM design along with the calculated controller parameters are now used to simulate the complete system. The stiffness and damping parameters as well as the system's dynamic response are verified using the simulation.

A rotor is now designed with the physical sizes obtained from the EM design. Dynamic analyses are performed on the rotor, using the verified stiffness and damping parameters, in order to obtain the rotor forces and displacements in the magnetic bearings. These results are compared to the maximum load capacity and allowable displacement due to the bearing geometry. The electromagnetic design is reviewed and the process is repeated until these parameters are within range when focus shifts to the rotordynamic performance.

The rotor design is reviewed until both the magnetic bearing locations as well as the rotor response are within range. The rotor forces and displacements are again verified and once the rotordynamic performance is within range, the design can be implemented. In the following sections the final iteration of the design process depicted in Figure 1 is discussed in detail.

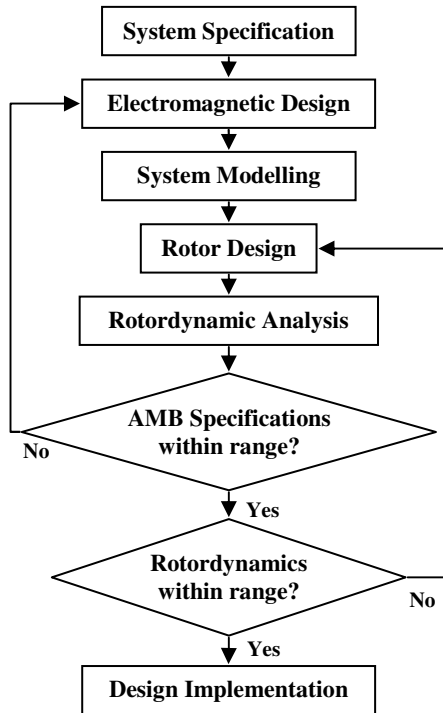


Figure 1: Iterative design process.

1 System specification

A flexible rotor must be designed that has a maximum operating speed of 10,000 rpm. The rotor should pass through its first three critical frequencies of which the first is the first bending mode before reaching maximum operating speed. The AMB must be able to stably suspend the flexible rotor through these critical frequencies and allow for advanced control implementation.

2 Electromagnetic design

The electromagnetic design is performed using MathCAD[®] software which allows the designer to easily adjust variables and reduce the time it takes to obtain the optimal design. The design is based on the heteropolar radial bearing design process outlined in [4]. Figure 2 shows the standard 8 pole heteropolar bearing geometry with the following simplifying design choices:

- Poles are paired which implies no flux splitting (NNSNNSS) and simplified control
- Quadrant control is implemented, i.e. each pole pair (NS) is wound in series
- Removable coils are used

The power amplifier (PA) specifications are obtained from the maximum force slew rate needed to implement the desired control. A 3 kVA (300 V, 10 A) PA specification is obtained and since a simple proportional derivative (PD) controller is implemented, the PA must be current controlled.

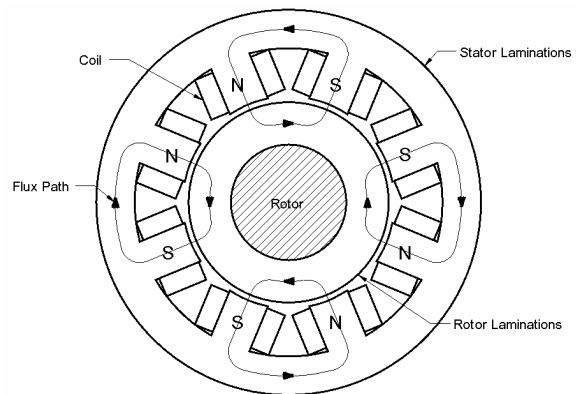


Figure 2: Standard 8-pole heteropolar radial bearing [4].

A maximum load capacity per unit area constraint is placed on an AMB due to material properties such as flux saturation and maximum current density. This implies that the peak load capacity dictates the pole face area. This serves as a point of departure for the journal and stator design. The maximum load capacity for one pole pair is obtained from Equation (1):

$$F = \frac{\mu_0 N^2 i_m^2 A_g}{x_s^2} \cos(\theta) \quad (1)$$

with μ_0 the permeability of free space, N the number of coil turns per pole, i_m the coil current, A_g the pole face area and x_s the air gap length. The angle θ is the pole angle with respect to the pole pair centre [4]. The AMB specifications obtained from the final design iteration are summarised in Table I.

Table I: AMB Specifications.

Parameter	Specification	Description
F_{max}	500 N	Maximum load capacity
dF/dt	5×10^6 N/s	Force slew rate
g_0	0.6 mm	Nominal air gap
k_{eq}	500 N/mm	Equivalent stiffness
b_{eq}	2.5 N.s/mm	Equivalent damping
A_g	689×10^{-6} m ²	Pole face area

2.3 Controller design

By utilising simple PD control an AMB emulates spring mass damper behaviour [5] with the equivalent stiffness and damping as given by Equations (2) and (3) respectively.

$$k_{eq} = 2K_p k_i - 2k_s \quad (2)$$

$$b_{eq} = 2K_D k_i \quad (3)$$

k_i and k_s , given by Equations (4) and (5) respectively, represent linearised system gains at the operating point of

i_0 and g_0 and K_P and K_D are the respective proportional and differential controller gains.

$$k_i = \left. \frac{\partial F}{\partial i_m} \right|_{i_m=i_0, x_s=g_0} = 2 \frac{\mu_0 N^2 i_0 A_g}{g_0^2} \cos(\theta) \quad (4)$$

$$k_s = \left. \frac{\partial F}{\partial x_s} \right|_{i_m=i_0, x_s=g_0} = -2 \frac{\mu_0 N^2 i_0^2 A_g}{g_0^3} \cos(\theta) \quad (5)$$

2.4 System modelling

In the process of designing and implementing a controller for a system such as an AMB an accurate model of the system becomes an invaluable tool. Figure 3 displays the nonlinear model that was used to simulate the system in MATLAB®. The simulation program contains the nonlinear force relationship and accurately simulates the switch-mode PA switching at 100 kHz.

The equivalent bearing stiffness and damping are verified using the simulation. The bearing stiffness is obtained from a steady-state condition by implementing a constant disturbance force and measuring the displacement. The bearing stiffness and damping parameters can also be determined from a step response using Equations (6) and (7) [6].

$$k_{eq} = \omega_n^2 m \text{ [N/m]} \quad (6)$$

$$b_{eq} = \zeta (2\sqrt{k_{eq} \cdot m}) \text{ [N.s/m]} \quad (7)$$

The damping factor (ζ) is obtained from the percentage overshoot ($P.O.$) and used in conjunction with the settling time to determine the system's natural frequency (ω_n).

2.5 Rotor design and dynamic analysis

In mathematical terms a natural frequency is an eigenvalue and a mode shape is an eigenvector. A distributed mass-elastic system has an infinite number of

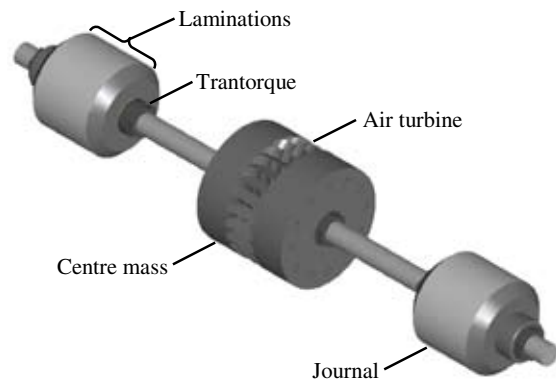


Figure 4: Flexible rotor CADKEY® model.

eigenvalues and associated eigenvectors in theory, but in practice only the lowest three or four critical speeds and associated whirl modes are excited in the operating speed range of a high speed machine [7]. Mode shapes are determined by the distribution of mass and stiffness along the rotor, as well as the bearing support stiffness. Figure 4 displays the CADKEY® model of the flexible rotor. The centre mass is used to lower the third critical frequency to below the maximum operating speed.

The first three critical speeds typically vary with support stiffness, as shown by the critical speed map in Figure 5. This undamped lateral critical speed map was generated with Dyrobes® software. The insensitivity of the third critical speed to support stiffness allows a range of operating speeds that does not traverse any of the critical speeds indicated by the vertical arrow in Figure 5. This is good machine design practice from a rotordynamics standpoint. The modern trend toward higher speeds however makes it difficult to avoid approaching or traversing the third critical speed [7]. For an equivalent stiffness of 500 N/mm and damping of 2.5 N.s/mm the first, second and third critical frequencies are situated at 2,947 rpm, 4,637 rpm and 7,276 rpm respectively.

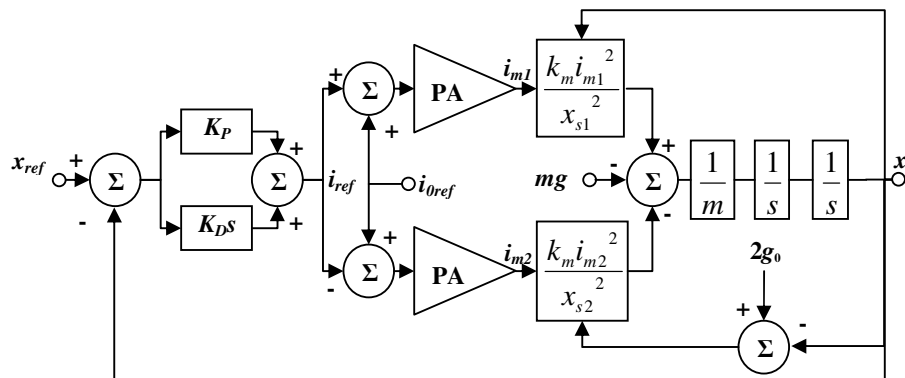


Figure 3: Simulation block diagram.

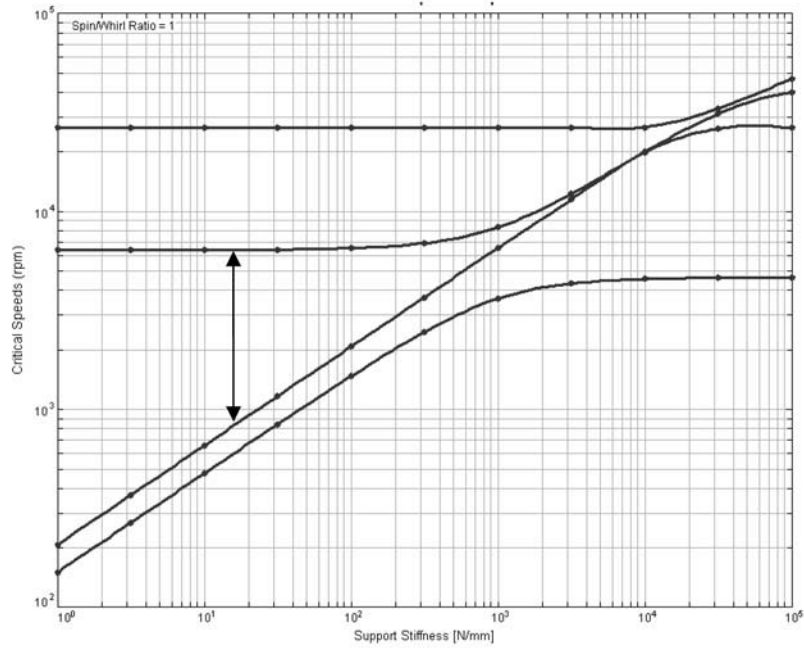


Figure 5: Critical speed map.

3. SYSTEM CHARACTERISATION

3.1 Equivalent stiffness and damping

Figure 6 shows the experimental and simulated results for a 50 μm step in the positive horizontal direction. Initially discrepancies were noted in the rise times and *P.O.* of the simulated and experimental responses. This was due to an unmodelled pole included in the differentiator path. With the additional pole introduced into the simulation, the simulated and experimental results correlate much closer as shown in Figure 6. From this response the following parameters are obtained: $k_{eq} = 1.654 \times 10^6$ N/m and $b_{eq} = 2.843 \times 10^3$ N.s/m. The corresponding critical frequencies obtained from the critical speed map (Figure 5) are estimated at 4,000 rpm, 8,200 rpm and 9,800 rpm.

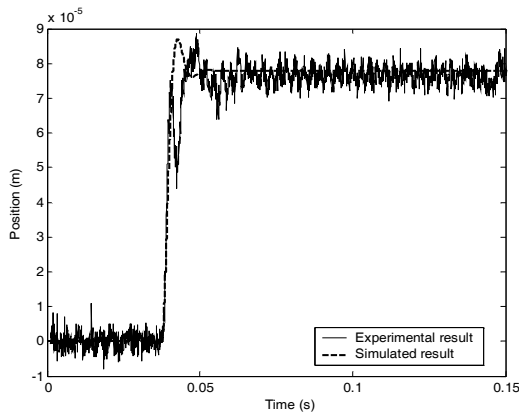


Figure 6: Horizontal step response.

3.2 Rotordynamic performance

The rotordynamic performance is experimentally determined by measuring rotor peak-to-peak displacement at the bearing locations as well as the centre mass during rotor acceleration. When comparing the vertical results of the right bearing shown in Figure 7 (a) to the predicted critical frequencies in Section 3.1, remarkable correlation is observed. This confirms the high equivalent stiffness value predicted by the simulation.

4. REVIEWING THE DESIGN PROCESS

The system design constitutes electromagnetic design, detailed system analysis and modelling. In the analytical analyses of the electromagnetic design no consideration is

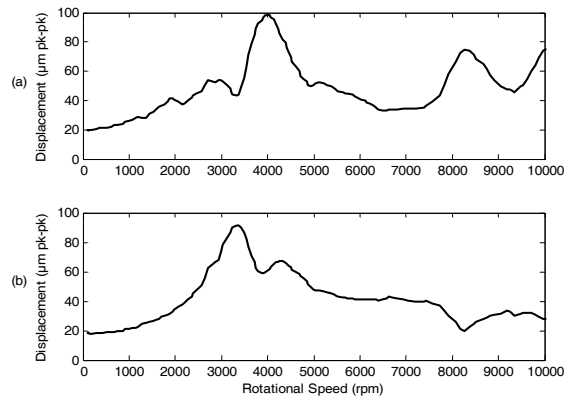


Figure 7: Right bearing (a) vertical, (b) horizontal displacement vs. rotational speed.

given to losses, leakage and fringing effects encountered in the electromagnetic circuit. The need for a detailed design process incorporating an analytical design, finite element method (FEM) design verification, detailed loss predictions and a detailed system simulation is apparent.

Future work is needed to include unmodelled dynamics e.g. the additional pole in the differentiator path in the analytical model of the AMB system. The analytical and simulation models may also be further refined to include actual system dynamics and nonlinearities currently not modelled e.g. magnetic material properties. A more comprehensive analytical and simulation model would have predicted the much higher equivalent stiffness of the actual system before design implementation.

5. CONCLUSIONS

The objective was to develop a design process for developing a flexible rotor double radial active magnetic bearing system. The design process was realised and verified through simulation and experimental results. This study highlights the importance of accurate modelling and the need for an integrated design tool incorporating aspects of FEM design verification, detailed loss predictions and detailed system simulation.

6. REFERENCES

- [1] M.E.F. Kasarda: "An Overview of Active Magnetic Bearing Technology and Applications", *The Shock and Vibration Digest*, Vol. 32 No. 2, pp. 91-99, March 2000.
- [2] L. Shi, L. Zhao, G. Yang, H. Gu, X. Diao, S. Yu: "Design and experiments of the active magnetic bearing system for the HTR-10", *2nd international topical meeting on high temperature reactor technology*, Paper D04, Beijing, China, Sept. 2004.
- [3] T. Takizuka, S. Takada, X. Yan, S. Kosugiyama, S. Katanishi, K. Kunitomi: "R&D on the power conversion system for gas turbine high temperature reactors", *Nuclear Engineering and Design*, Vol. 233 No. 1-3, pp. 329-346, October 2004.
- [4] P. Allaire, C.R. Knospe, *et al*: "Short course on magnetic bearings," Alexandria Virginia United States of America: University of Virginia, 1997.
- [5] G. Schweitzer, H. Bleuler, A. Traxler: *Active Magnetic Bearings: Basics, Properties and Applications of Active Magnetic Bearings*, Authors Reprint, Zürich, 2003.
- [6] Richard C. Dorf, Robert H. Bishop: *Modern Control Systems*, Prentice Hall, New Jersey, Ninth Edition, pp. 36-47, pp. 227-233, 2001.
- [7] John M. Vance: *Rotordynamics of Turbomachinery*, WILEY, New York, pp. 116-170, 1988.

AN ADAPTIVE HYBRID LIST DECODING AND CHASE-LIKE ALGORITHM FOR REED-SOLOMON CODES

W. Jin, H. Xu and F. Takawira

School of Electrical, Electronic and Computer Engineering, University of KwaZulu-Natal, Howard College Campus, King George V Avenue, Durban 4041, South Africa

Abstract: This paper presents an adaptive hybrid Chase-like algorithm for Reed-Solomon codes, which is based on the list decoding algorithm. The adaptive hybrid algorithm is based on the reliability threshold to exclude the more reliable bits from being processed by the list decoding algorithm and reduce the complexity of the hybrid algorithm. Simulation results show that the decoding complexities of the adaptive hybrid algorithm for both (15.7) and (31.21) Reed-Solomon codes are almost the same as those of the list decoding algorithm (without Chase algorithm) at high signal-to-noise ratios, but there is a significant improvement in FER performance.

Key words: The list decoding algorithm, Bit reliability, Adaptive scheme, Hybrid algorithm.

1. INTRODUCTION

How to approach the performance of the Maximum likelihood decoding (MLD) with less complexity is a subject which has been researched extensively, especially for Reed-Solomon (RS) codes which are powerful error-correcting codes in digital communications and digital data-storage systems. Applying the bit reliability obtained from the channel to the conventional decoding algorithm is always an efficient technique to achieve the performance of the MLD, although the exponential increase of complexity is always concomitant. In [1]-[2], the authors also use the bit reliability to improve the performance of Bose-Chaudhuri-Hocquenghem (BCH) codes and RS codes, respectively. It is undoubted that improved performance can be achieved if we apply the bit reliability to an enhanced algebraic decoding algorithm that is more powerful than the conventional algebraic decoding algorithms.

The Guruswami-Sudan (GS) list decoding algorithm [3] that was discovered by Madhu Sudan in 1997 and developed by Guruswami and Sudan two years later [4] is one of the enhanced algebraic decoding algorithms for RS codes. In the GS list decoding algorithm, the number of errors that can be corrected increases to $t_{GS} = n-1 - \lfloor \sqrt{(k-1)n} \rfloor$ for (n, k) RS codes, where $\lfloor x \rfloor$ is the integer of x . It is easy to show that the GS list decoding algorithm is able to correct more errors than the conventional algebraic decoding algorithms. The fundamental idea of the GS algorithm is to take advantage of an interpolation step to get an interpolation polynomial which is produced by the support symbols, the received symbols and their corresponding multiplicities. The GS algorithm then implements a factorisation step to find the roots of the interpolation

polynomial. After comparing the reliability of these codewords, which are obtained from the output of factorisation, the GS algorithm outputs the most likely one. The support set, the received set and the multiplicity set are created by the Koetter-Vardy (KV) algorithm [5] that is a practical implementation of the GS algorithm.

To further improve the performance of the GS list decoding algorithm, [6] has proposed a hybrid list decoding and Chase-like algorithm. Simulation results in [6] show that the performance of the hybrid algorithm for the (7.5) RS code can approach that of the MLD, and the performance of the (15.7) RS code can correct one more symbol error than the GS list decoding algorithm. The complexity of the hybrid algorithm in [6] depends on the number of bits which are used in the Chase-like algorithm, but the complexity is exponential with the number of bits. Actually, as signal-to-noise ratio (SNR) increases the received bits are more reliable, and it is not necessary to apply the Chase-like algorithm in the GS list decoding algorithm. To further reduce the complexity at high SNRs, we propose an adaptive hybrid algorithm which is based on the GS list decoding and the adaptive Chase-like algorithm in this paper. The adaptive hybrid algorithm is based on the reliability threshold to exclude the more reliable bits from being processed by the GS list decoding algorithm.

This paper is organised as follows. Section 2 introduces the KV soft-decision front end along with the corresponding algorithm. Section 3 gives a brief description of the adaptive Chase-Generalised Minimum Distance (Chase-GMD) algorithm. Section 4 explains how the list decoding algorithm and the Chase algorithms can be combined with further incorporation of the adaptive idea. Simulation results are given in Section 5. Section 6 draws conclusions for this paper.

2. THE KOETTER-VARDY SOFT-DECISION FRONT END

Guruswami and Sudan hinted at a possibility of a soft-decision extension to their algorithm by allowing each point on the interpolated curve to have its own multiplicity. Koetter and Vardy (KV) proposed a method to perform soft-decision decoding by assigning unequal multiplicities to different points according to their relative reliabilities. An algorithm that generates the multiplicity matrix from the reliability matrix Π was presented in [5]. A lower complexity algorithm for implementing the KV front-end was proposed in [7], but we still use the KV algorithm from [5] which is shown as follows.

The KV Algorithm for calculating Multiplicity Matrix M from the reliability matrix Π subject to complexity constraint s .

Definition: $m_{i,j}$ is an entry at the position (i, j) in multiplicity matrix M .

Algorithm:

Choose a desired value $s = \sum_{i=0}^{q-1} \sum_{j=0}^{n-1} m_{i,j}$; $\Pi^* \leftarrow \Pi$;

$M \leftarrow 0$;

While $s > 0$ do

Find the position (i, j) of the largest entry $\pi_{i,j}^*$ in Π^* ;

$\pi_{i,j}^* \leftarrow \frac{\pi_{i,j}}{m_{i,j} + 2}$; $m_{i,j} \leftarrow m_{i,j} + 1$; $s \leftarrow s - 1$;

End while

Using this algorithm, we obtain the support set, the received set and the multiplicity set. The candidates of the codeword polynomial are obtained through an interpolation step and a factorisation step.

3. AN ADAPTIVE CHASE-GMD ALGORITHM

Mahran and Benasissa proposed an adaptive Chase-GMD algorithm for linear block codes in [8]. In the adaptive Chase-GMD Algorithm, an l -bit quantizer is used to classify the received bits by their reliability. A brief overview of the adaptive Chase-GMD algorithm is given as follows.

As errors are more likely to occur in the first η least reliable positions of the received bits R , the Chase-GMD algorithm is firstly considered to be applied in those positions. A reliability threshold function of confidence level, r , is used in the adaptive Chase Algorithm. The higher the confidence level the higher the possibility of selecting more chase-like erasures. The threshold function T is given by:

$$T = S \times r \times \sqrt{\frac{0.5}{\left(\frac{E_b}{N_o}\right) \cdot R_c}} \quad (1)$$

where R_c is the rate of the RS code. E_b / N_o is the bit signal-to-noise ratio. S given in (2) is a scalar constant that depends on the number of quantisation levels.

$$\frac{0.45}{2^{l-3}} \leq S \leq \frac{0.7}{2^{l-3}} \quad (2)$$

The threshold can be used to decide which bit should be processed by the Chase algorithm. Let the reliability of received sequence be α . The bits will be used in the adaptive Chase algorithm only if their reliabilities satisfy the following condition:

$$-T \leq \alpha_j \leq +T \quad j = 1, 2, \dots, \left\lceil \frac{d_{\min}}{2} \right\rceil \quad (3)$$

If a bit does not satisfy the above condition then it can be ignored by the Chase algorithm even if it is the most unreliable bit in the received bits.

4. THE ADAPTIVE HYBRID ALGORITHM

The application of the Chase algorithm to the KV soft-decision front end based on the bit reliability can improve the performance of the list decoding algorithm, with an adaptive scheme reducing complexity.

Before the presentation of the adaptive hybrid algorithm, there are some definitions which should be made clear. We can obtain the support set, the received set and the multiplicity set through the KV front end. We use 'multi-points' to define the received symbols whose support symbols are the same, 'low-multiplicity-points' to define the received symbols whose multiplicities are less than the maximum multiplicity except for multi-points, and 'high-multiplicity-points' to define the received symbols whose multiplicities are equal to the maximum multiplicity. We refer to the high-multiplicity-points as reliable points, and other received symbols as unreliable points.

Now, the adaptive hybrid list decoding and the Chase-like algorithm contain the following steps:

- i. Implement the KV soft-decision front end to obtain the support set, the received set and the multiplicity set.
- ii. Use Equation (1) to obtain the threshold value with appropriate scale constant S and confidence level r .
- iii. Calculate the number of multi-points in the output of the KV soft-decision front end. If more than one received symbol is found to have the same support symbols, the number of multi-points increases by one. We denote it as N_{multi} .

- iv. Calculate the number of low-multiplicity-points in the output of the KV soft-decision front end. We denote it as N_{low} .
- v. If $N_{multi} + N_{low} \leq t_{GS}$
 - use the chase-like algorithm for high-multiplicity-points. The threshold can be used to finally decide if those unreliable bits are picked up by the Chase algorithm or not.
 - Else
 - use the Chase-like algorithm for both low-multiplicity-points and high-multiplicity-points. The unreliable bits selected by the Chase algorithm must also satisfy the condition mentioned above.

t_{GS} is the number of errors that can be corrected for (n, k) RS codes.
- vi. Output all the received sets, the corresponding support set and multiplicity set to interpolation step.
- vii. Interpolation step proposed in [5].
- viii. Factorisation step proposed in [5].
- ix. Compare the probability of all candidates of the codeword created by different received sets and output the most likely one.

In the above proposed algorithm, we do not consider the multi-points because the list decoding algorithm has already taken them into account. In other words, the list decoding algorithm pays more attention to multi-points than other points. When the list algorithm fails, the errors coming from multi-points are not the significant source of failure for the list decoding.

In the above algorithm, we classify the output of the KV soft-decision front end into two different cases, $N_{multi} + N_{low} \leq t_{GS}$ and $N_{multi} + N_{low} > t_{GS}$. We will discuss them separately.

If $N_{multi} + N_{low} \leq t_{GS}$, it means that the number of unreliable points does not exceed the error-correcting ability. Even if all unreliable symbols are incorrect, the list decoding algorithm can still generate the right codeword polynomial. In this case, the errors coming from reliable symbols are the main reason for the failure of the list decoding algorithm, so we apply the Chase algorithm to reliable symbols in order to obtain more reliable received sets corresponding to the same multiplicity.

If $N_{multi} + N_{low} > t_{GS}$, it means that the number of unreliable symbols exceeds the error-correcting ability. If all these symbols are incorrect, the list decoding algorithm can not generate the right codeword polynomial. In this case, we have to concentrate on both low-multiplicity-points and high-multiplicity-points.

Because the list decoding algorithm has already taken the multi-points into account, we do not take the multi-points into account. Before we apply the Chase algorithm to both kinds of points, we must make it clear which kind of points we should take into account first, low-multiplicity-points or high-multiplicity-points. We can extend the search scope into high-multiplicity-points by changing the unreliable bits. In order to improve the search scope, changing the unreliable bits in high-multiplicity-points is better than in low-multiplicity-points. This implies that we can obtain more candidate codeword polynomials if we choose high-multiplicity-points. It seems that we should change unreliable bits in high-multiplicity-points, but at high SNRs, we draw a different conclusion. As the SNR increases, the high-multiplicity-points (reliable points) become more and more 'reliable'. The probability that reliable points are received correctly is very large. The performance improvement is marginal even if we invert these bits which are in the reliable points. In this paper, we only take into account low-multiplicity-points first at high SNRs.

There are several threshold values that are shown in Figure 1 and Figure 2 for $R_c = 0.467$. The scalar constant in Figure 1 is 0.225, which is the minimum of a 4-bit quantizer. The scalar constant in Figure 2 is 0.35, which is the maximum of the same 4-bit quantizer.

It is obvious that we can change the confidence level to get different thresholds. As the confidence level increases, the number of bits that can be ignored by the Chase algorithm decreases. The confidence level can be adjusted to fit the list decoding algorithm. It is expected that the performance of the adaptive hybrid algorithm is comparable with the performance of the hybrid Chase-list algorithm in [6], but with lower complexity.

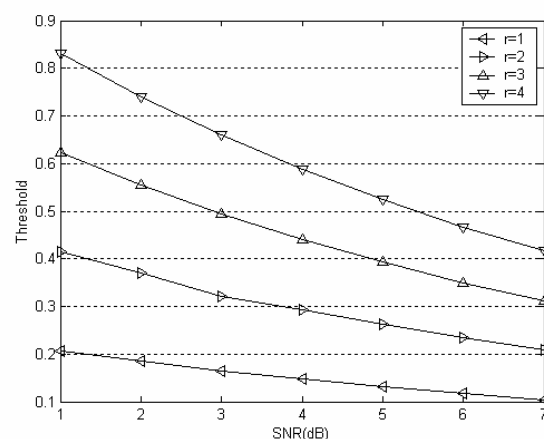


Figure 1: The thresholds with $S=0.225$ for $R_c = 0.467$.

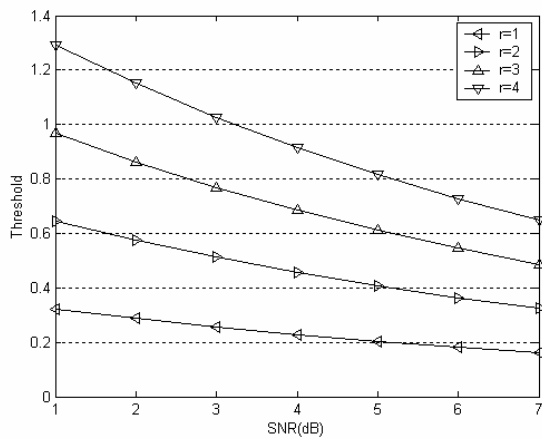


Figure 2: The thresholds with $S=0.35$ for $R_c = 0.467$.

5. SIMULATION RESULTS

All simulations are performed in an AWGN channel and BPSK transmission is assumed. For comparison purposes, we simulate the conventional decoding, the list decoding, the hybrid algorithm in [6] and the adaptive hybrid algorithm. We use the Chase-2 algorithm to improve the performance for the (15.7) RS code. We select 4 unreliable bits according to the least reliable positions based on the hybrid algorithm. A 4-bit quantizer with the confidence level 1 to 8 is used. In the simulation of the (15.7) RS code we choose $S=0.26$ and $r=3$, which are suitable for the list decoding algorithm with maximum multiplicity 2. The frame error rate (FER) performance is shown in Figure 3, and the corresponding complexity is shown in Figure 5. The simulation results of 2-bit hybrid algorithm, 3-bit hybrid algorithm and 4-bit hybrid algorithm are also shown in those figures for comparison. Based on the fact that one interpolation step and one factorisation step take almost 95% of total decoding time, we define a unit of the decoding complexity as the time taken by one interpolation step and one factorisation step in the list decoding algorithm. The hybrid algorithm can correct one more symbol error than the list decoding algorithm. Figure 5 also shows that the complexity of the adaptive hybrid algorithm decreases as the SNR increases. The complexity of the adaptive hybrid algorithm at 7dB is almost 2, which is the complexity with the 1 bit Chase-2 algorithm applied to the list decoding algorithm, but the gap between the FER performance of the adaptive hybrid algorithm and the hybrid's is negligible.

We still use the Chase-2 algorithm to improve the performance for the (31.21) RS code. A 4-bit quantizer is also used with $S=0.225$ and $r=3$. The FER performance is shown in Figure 4, and the corresponding complexity is shown in Figure 6. The simulation results of the 1-bit hybrid algorithm and the 2-bit hybrid algorithm are also shown in those figures for comparison. The simulation

results in Figure 4 and Figure 6 show that the adaptive algorithm can reduce the complexity with small or marginal performance penalty. The complexity of the adaptive hybrid algorithm in Figure 6 can approach the list decoding algorithm without the Chase algorithm at high SNRs.

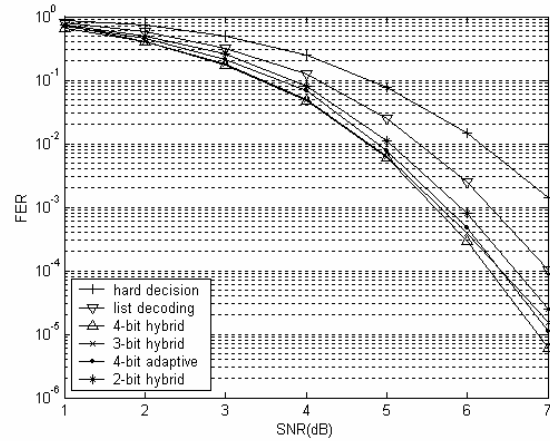


Figure 3: FER performance of the (15.7) RS code.

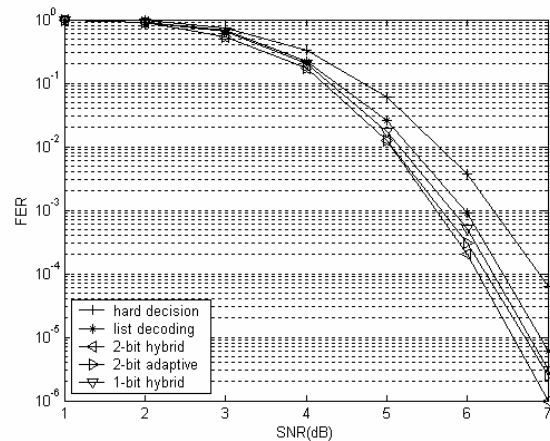


Figure 4: FER performance of the (31.21) RS code.

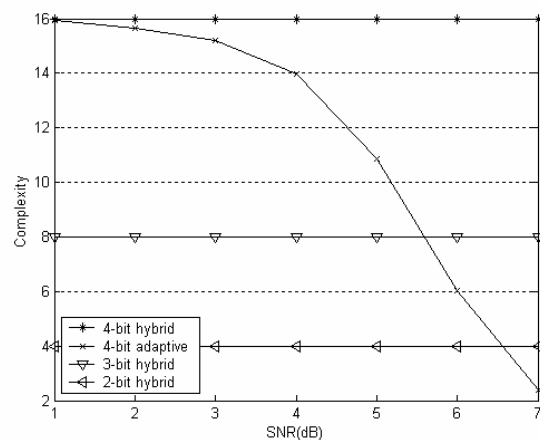


Figure 5: The complexity of the (15.7) RS code.

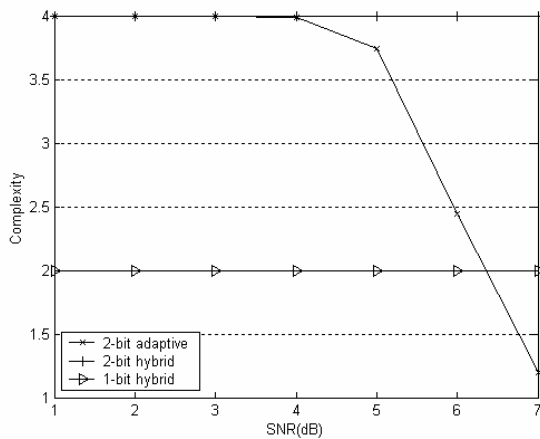


Figure 6: The complexity of the (31,21) RS code.

6. CONCLUSION

In this paper, an adaptive hybrid list decoding and Chase-like algorithm is presented. The adaptive hybrid algorithm is based on the reliability threshold to exclude the more reliable bits from being processed by the list decoding algorithm. In the above steps we obtain more received sets and accordingly obtain more candidate codeword polynomials. As the search scope is extended, the transmitted codeword is easily obtained. Simulation results show that the FER performance of the proposed adaptive hybrid algorithm for both (15,7) and (31,21) RS codes can be comparable with the performance of the hybrid algorithm in [6], but the complexity is much lower, especially at high SNRs.

7. REFERENCES

- [1] M. P. C. Fossorier and S. Lin: "Complementary reliability-based decoding of binary block codes", *IEEE Transactions on Information Theory*, Vol.43, pp. 1667~1672.
- [2] T. H. Hu and S. Lin: "An efficient hybrid decoding algorithm for Reed-Solomon codes based on bit reliability", *IEEE Transactions on Communications*, vol.51, no.7, pp. 1073~1081, July 2003.
- [3] M. Sudan: "Decoding of Reed Solomon codes beyond the error-correcting bound", *J. Complexity*, Vol. 13, pp.180~193, 1997.
- [4] V.Guruswami and M. Sudan: "Improved decoding of Reed-Solomon codes and algebraic geometry codes", *IEEE Transactions on Information Theory*, vol. 45 no. 6, pp. 1757~1767, Sept. 1999.
- [5] R. Koetter: "Fast generalized minimum-distance decoding of algebraic-geometry and Reed-Solomon codes", *IEEE Transactions on Information Theory*, vol. 42 no. 3, pp. 721~736, May 1996.
- [6] W. Jin, H. Xu and F. Takawira: "A hybrid list decoding and Chase-like algorithm of Reed-Solomon codes", *Proceedings of the 4th International Symposium on Information and Communication Technologies*, pp. 87~92, Jan 3-6 2005.
- [7] W. J. Gross, F. R. Kschischang, R. Koetter, and P. Gulak: "Simulation results for algebraic soft-decision decoding of Reed-Solomon codes", *Proceedings of the 21'st Biennial Symposium on Communications*, pp. 356~360, June 2-5 2002.
- [8] A. Mahran and M. Benaissa: "Adaptive combined Chase-GMD algorithms for block codes", *IEEE Communications Letter*, Vol.8, No.4, pp.235-237, April 2004.